Science Advances
AAAS

advances.sciencemag.org/cgi/content/full/5/4/eaav4310/DC1

Supplementary Materials for

A 192-heme electron transfer network in the hydrazine dehydrogenase complex

M. Akram, A. Dietl, U. Mersdorf, S. Prinz, W. Maalcke, J. Keltjens, C. Ferousi, N. M. de Almeida, J. Reimann, B. Kartal, M. S. M. Jetten, K. Parey*, T. R. M. Barends*

*Corresponding author. Email: krparey@biophys.mpg.de (K.P.); thomas.barends@mpimf-heidelberg.mpg.de (T.R.M.B.)

Published 17 April 2019, *Sci. Adv.* **5**, eaav4310 (2019)
DOI: 10.1126/sciadv.aav4310

The PDF file includes:

Other Supplementary Material for this manuscript includes the following:

(available at advances.sciencemag.org/cgi/content/full/5/4/eaav4310/DC1)

Supplementary Text

Structure of Kustc1130

The structure of Kustc1130 consists of two β-sheets comprising 7 strands in total, where strands 3 and 4 are connected by a disulfide bond (fig. S4A,B). A query for structurally similar protein folds using the Dali server (*39*) showed that this fold is similar to the C-terminal 7-stranded β-sandwich domain of carboxypeptidase D domain II or CPD II (PDB id: 1H8L; Z score=11.0; RMSD=2.7 Å and identity=24 %). This domain, in turn, is similar to transthyretin (pre-albumin) and sugar binding proteins (*40*), however, no functional significance of the domain has been defined so far. Interestingly, another hit was carboxypeptidase M (CPM) C-terminal β-sandwich domain (PDB id: 1UWY; Z-score= 9.6; RMSD= 2.0 and identity= 22 %). CPM is an extracellular glycosylphosphatidyl-inositol (GPI) anchored membrane glycoprotein (*41*). The GPI anchor segment starts after the last β-strand and spans 45 amino acids as random coil possessing a GPI-anchor motif (PDHSAA). When aligned with the Kustc1130 structure this part covers only 9 residues (Lys106 to His114) in Kustc1130. Many of the other significant hits are cell-adhesion proteins such as the CNA_2 domain (RMSD = 1.9 Å and identity only 13%) of the pilus component BcpA from *Bacilllus cereus* (*42, 43*) and the fibronectin-adhesion protein Fba-B (RMSD = 1.9 Å and identity only 13%) responsible for invasion of endothelial cells by *Streptococcus pyogenes* (*44*). The domain III of pyrogallol–phloroglucinol transhydroxylase (RMSD = 1.6 Å; identity = 18 %) from the anaerobic bacterium *Pelobacter acidigallici* is also proposed to be associated with the cytoplasmic membrane (*45*). However, no features related to any type of membrane protein (integral or peripheral) could be located on the Kustc1130 sequence.

Single-particle cryo-EM reconstructions of HDH assemblies

We performed cryo-EM reconstructions of four- and five-fold symmetrical *K. stuttgartiensis* HDH particles prepared by crosslinking under high-salt conditions as well as of fourfold symmetrical particles prepared without crosslinking at high salt concentration. The crosslinking conditions were those we previously used to prepare samples for negative stain EM (*7*) and which were chosen to maximize the amount of four- and five-fold particles that had been observed in smaller amounts without crosslinking under low-salt conditions. During gel filtration, the elution volume of the crosslinked species was identical to the elution volume of the high-molecular weight species observed in native HDH under the high salt conditions (150 mM KCl). The UV-Vis spectrum of the crosslinked material was identical to that of native HDH and successful crosslinking was confirmed by 4-10% SDS-PAGE resulting in a single band at the top of the separating gel. We therefore concluded that the purified crosslinked species correspond to the high-molecular weight species observed in native HDH and do not contain artificial aggregates. Our cryo-EM maps of the crosslinked and non-crosslinked four-fold symmetrical particles are at 5.2 and 5.5 Å resolution, respectively (fig. S1), and show these particles to be identical to the HDH assembly found in the asymmetric unit of the crystal structure (fig. S2), apart from the absence of the Kustc1130 molecules, whereas our 6.2 Å resolution cryo-EM map of the five-fold symmetrical particles revealed a "decamer of trimers", $(\alpha_3)_{10}$, arrangement consisting of two pentameric rings of HDH trimers (fig. S1, S7).

Interestingly, the interfaces between HDH trimers in the $(\alpha_3)_8$ and $(\alpha_3)_{10}$ complexes are extremely similar (fig. S8), the differences being caused by minor differences in relative orientation of the interacting trimers in a manner reminiscent of the quasi-equivalence principle guiding virus

assembly (*46*). Because of this, formation of the $(\alpha_3)_{10}$ complex also buries the heme 1 groups, resulting in the formation of an extended heme network of in this case 240 heme groups (fig. S7C,D), illustrating the propensity of HDH to form such large, extended heme networks.

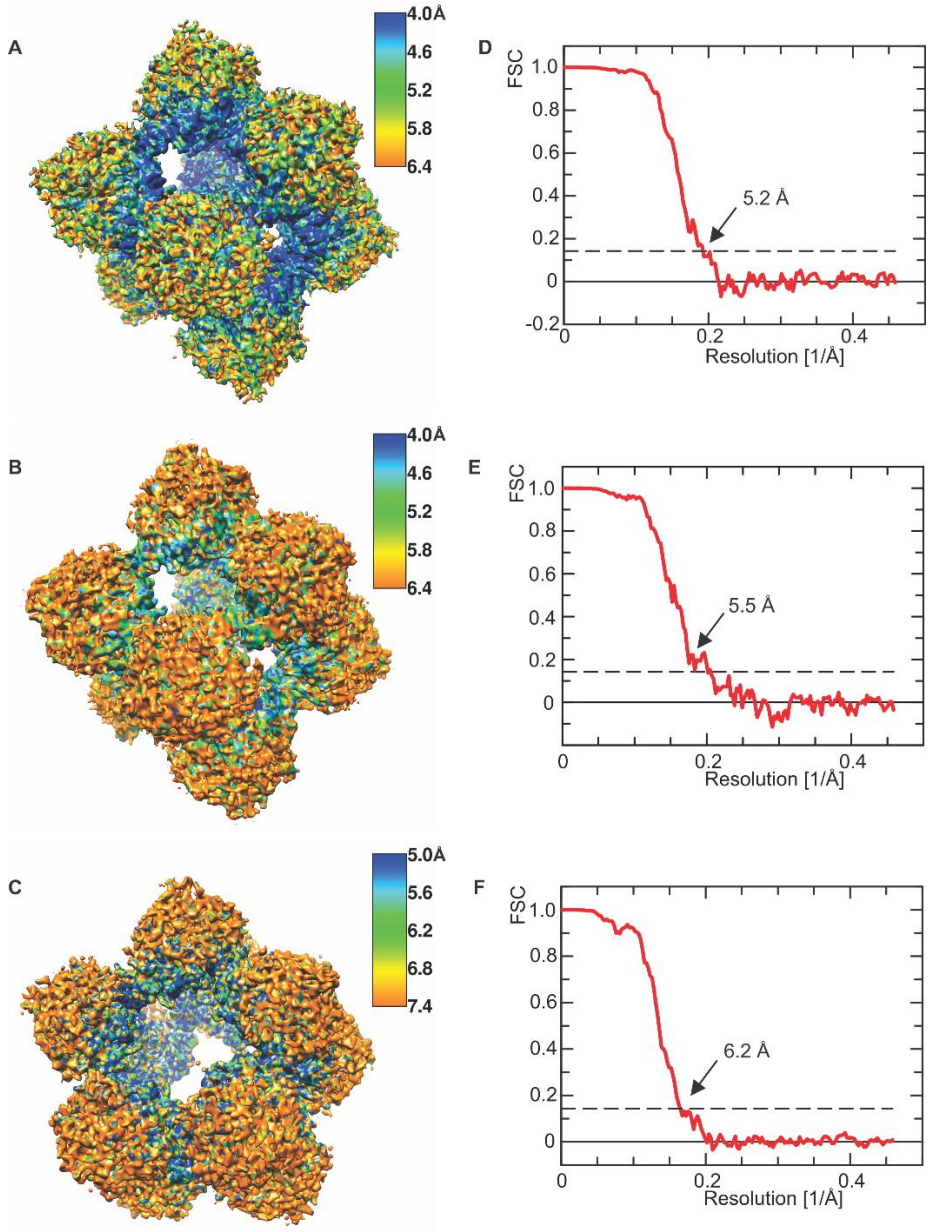

Fig. S1. Single-particle cryo-EM map quality. A,B,C. Local resolution of the maps for the crosslinked fourfold-, the non-crosslinked fourfold- and crosslinked five-fold symmetrical particles, respectively, as analyzed by ResMap (*37*). D,E,F. Fourier shell correlation calculated between two independently refined half maps (*36*) vs. resolution for the maps of the crosslinked fourfold-, the non-crosslinked fourfold and the crosslinked five-fold symmetrical particles, respectively. The map resolution (arrow) is indicated at the point where the FSC drops below the 0.143 threshold, which is shown by the dashed line (*35*).

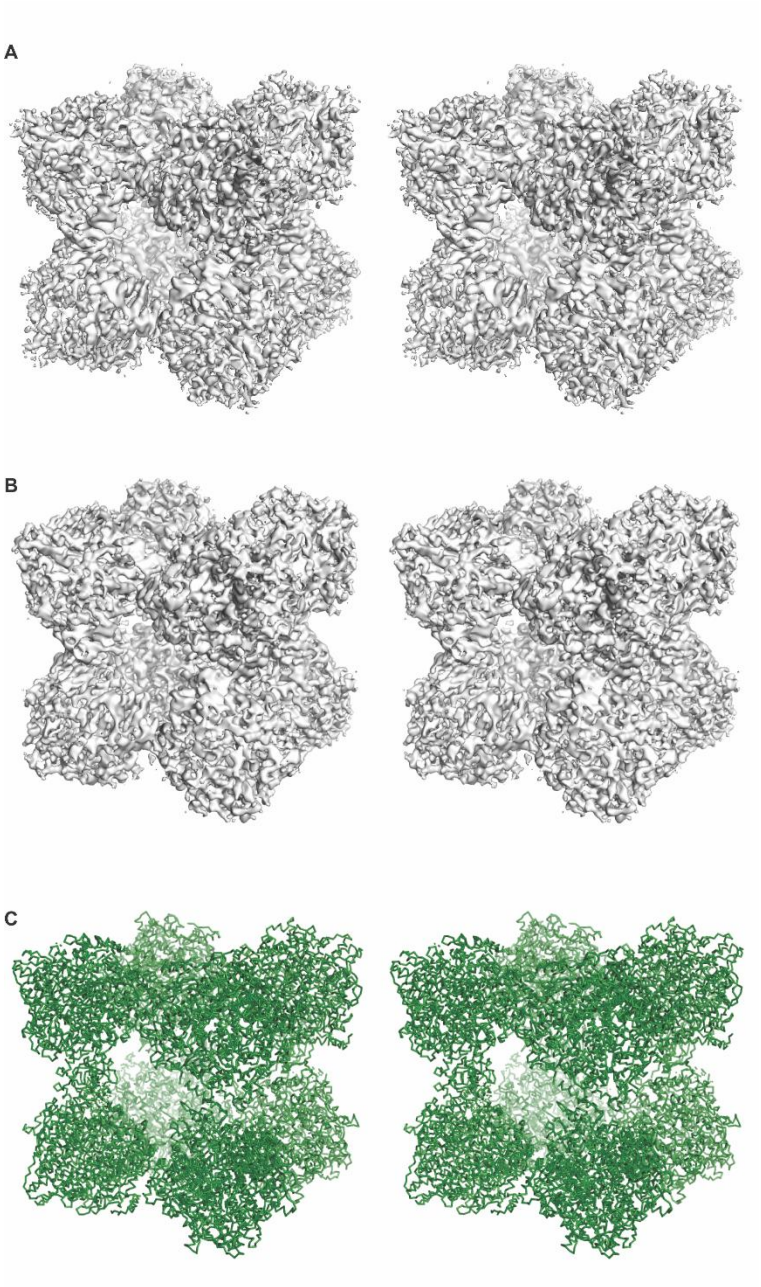

Fig. S2. Single-particle cryo-EM of HDH. A. Stereo view of the 5.2 Å resolution cryo-EM map of cubic particles of *K. stuttgartiensis* HDH prepared by crosslinking under high-salt conditions. B. Stereo view of the 5.5 Å resolution cryo-EM map of cubic particles of *K. stuttgartiensis* HDH prepared under high-salt conditions without crosslinking. C. Stereo view of the Cα trace of HDH monomers in the cubic assembly in the asymmetric unit of the *K. stuttgartiensis* HDH crystal structure.

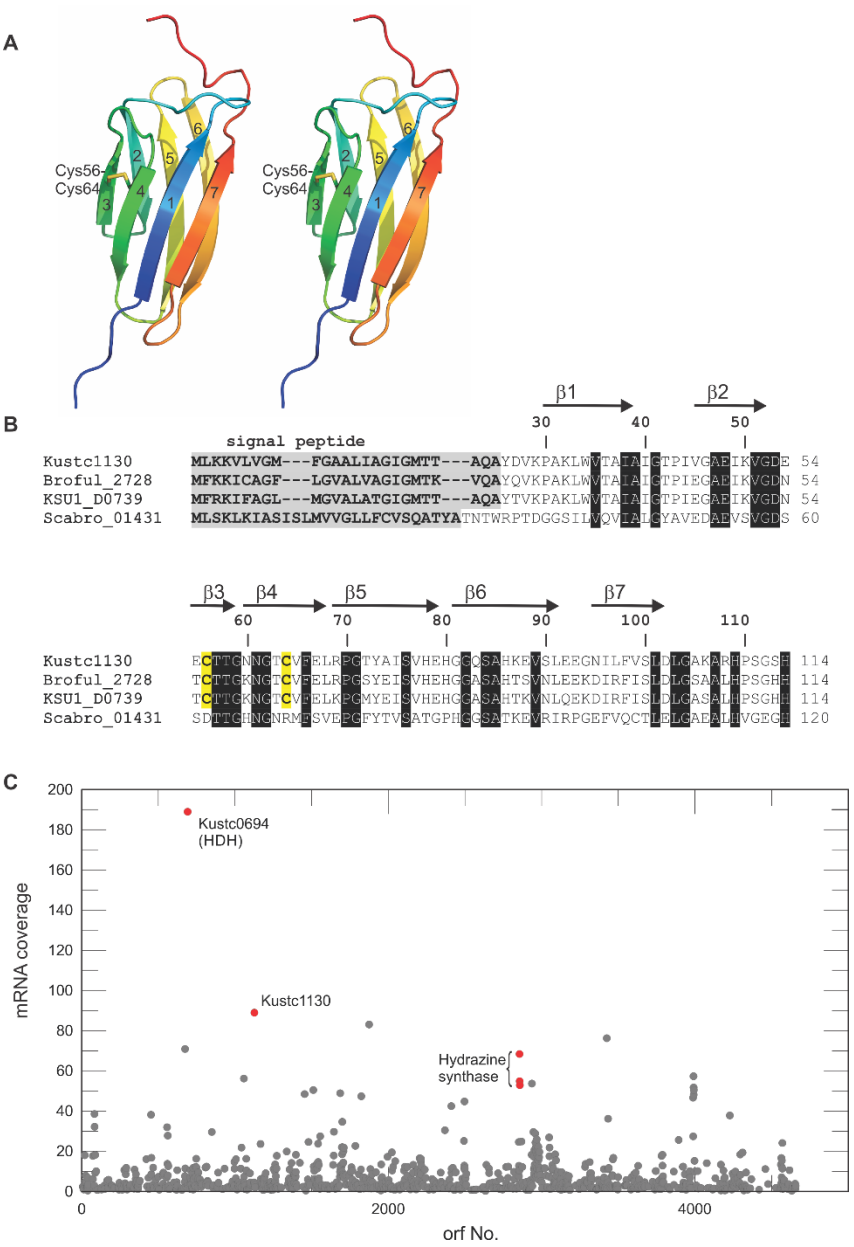

Fig. S3. Details of the assembly factor Kustc1130. A. Stereo view of the fold of Kustc1130, colored from blue at the N-terminus to red at the C-terminus, and the individual β strands are numbered. The disulfide bridge between Cys56 on strand β3 and Cys64 on strand β4 is shown as sticks. B. Alignment of the sequence of Kustc1130 with the closest homologs in *Brocadia fulgida* (Broful_2728), *Jettenia caeni* (KSU1_D0739) and *Scalindua brodae* (Scabro01431). The identity with the first two proteins is >70% whereas that with the *Scalindua* homolog is only 34%. The disulfide-forming cysteines are conserved in the orthologues from fresh water anammox genera (*Kuenenia*, *Brocadia* and *Jettenia*) but are absent in the marine anammox genus *Scalindua*. C. Scatter plot of the mRNA coverage of ORFs of *K. stuttgartiensis*. The mRNA coverage of Kustc1130 and HDH as well as the three subunits of hydrazine synthase are marked in red. The data displayed in the graph are from (*47*).

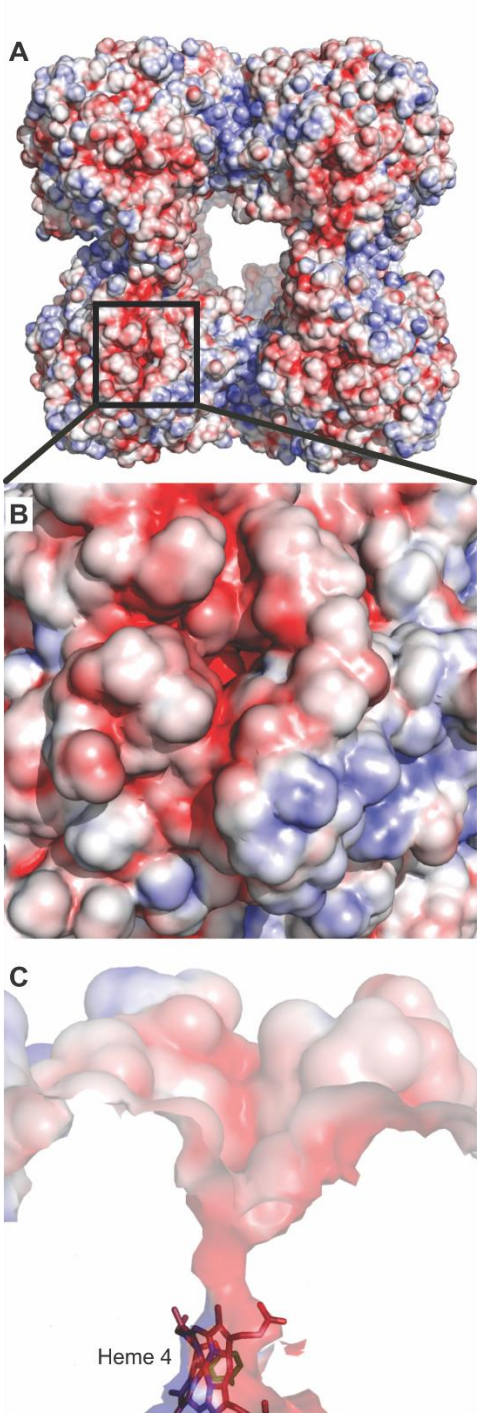

Fig. S4. Electrostatics of HDH complex. A. Electrostatic surface potential of the HDH complex, colored from -10 k_bT/e (red) to +10 k_bT/e (blue). B. Zoomed-in view showing the surroundings of the tunnel to one of the active sites. C. Side view of the tunnel leading towards one of the active site hemes 4.

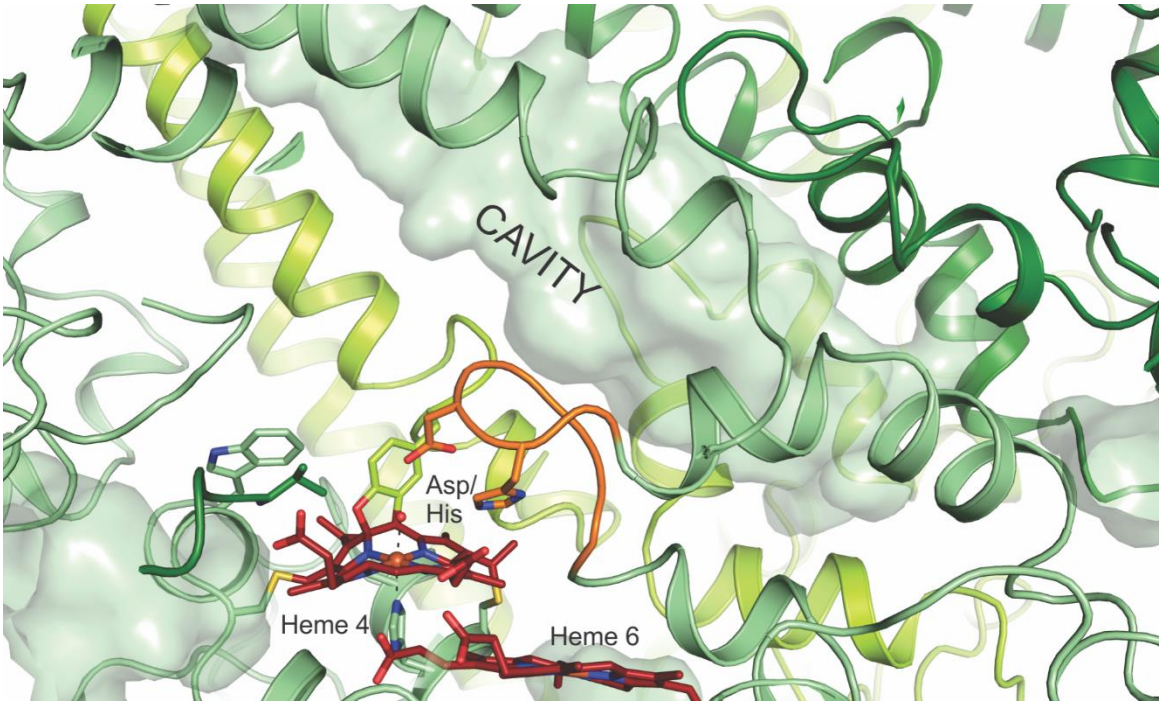

Fig. S5. Central cavity in HDH trimers. A large cavity lies directly behind the loop containing the conserved Asp/His pair (orange). Protons abstracted from the hydrazine substrate at the active site heme 4 could be transferred to water molecules occupying this cavity.

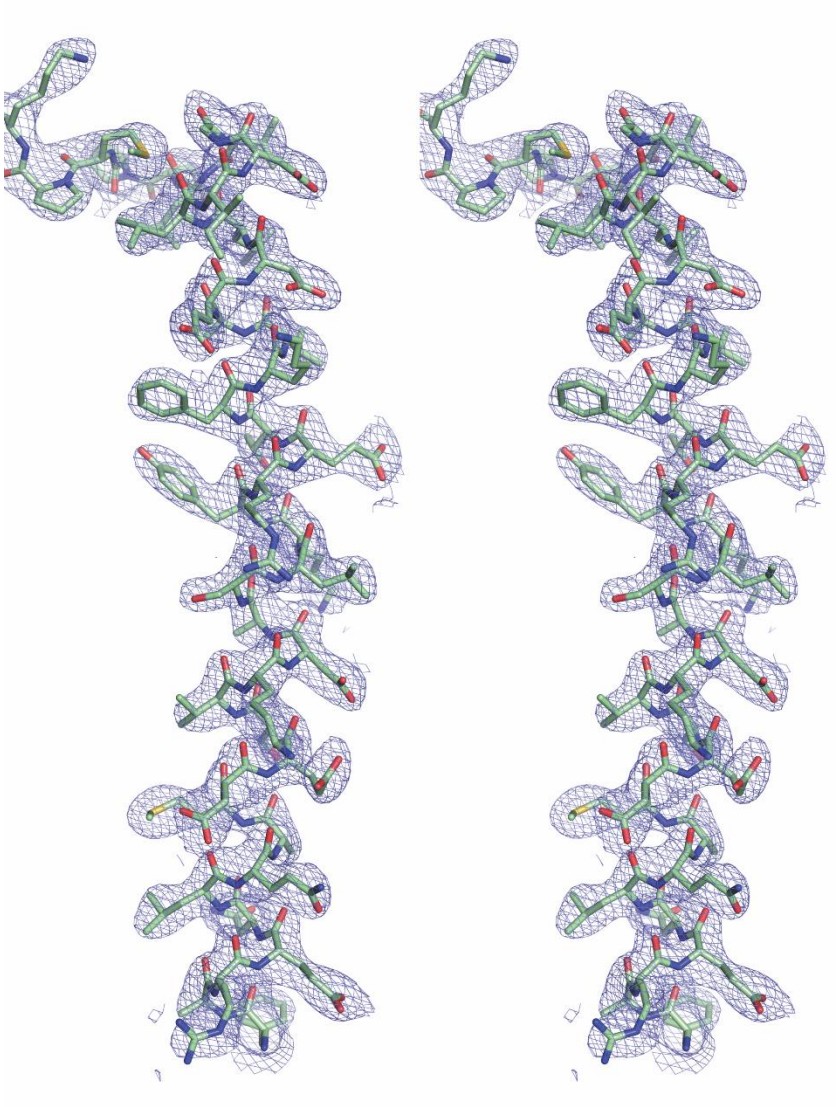

Fig. S6. Stereo figure showing the quality of the crystallographic electron density map. The 2*m*Fo-*D*Fc(*48*) electron density map (blue mesh) is contoured at 1.0 σ and overlaid on the final, refined crystal structure (shown: residues 350 to 390 of HDH molecule "G" in the crystal structure).

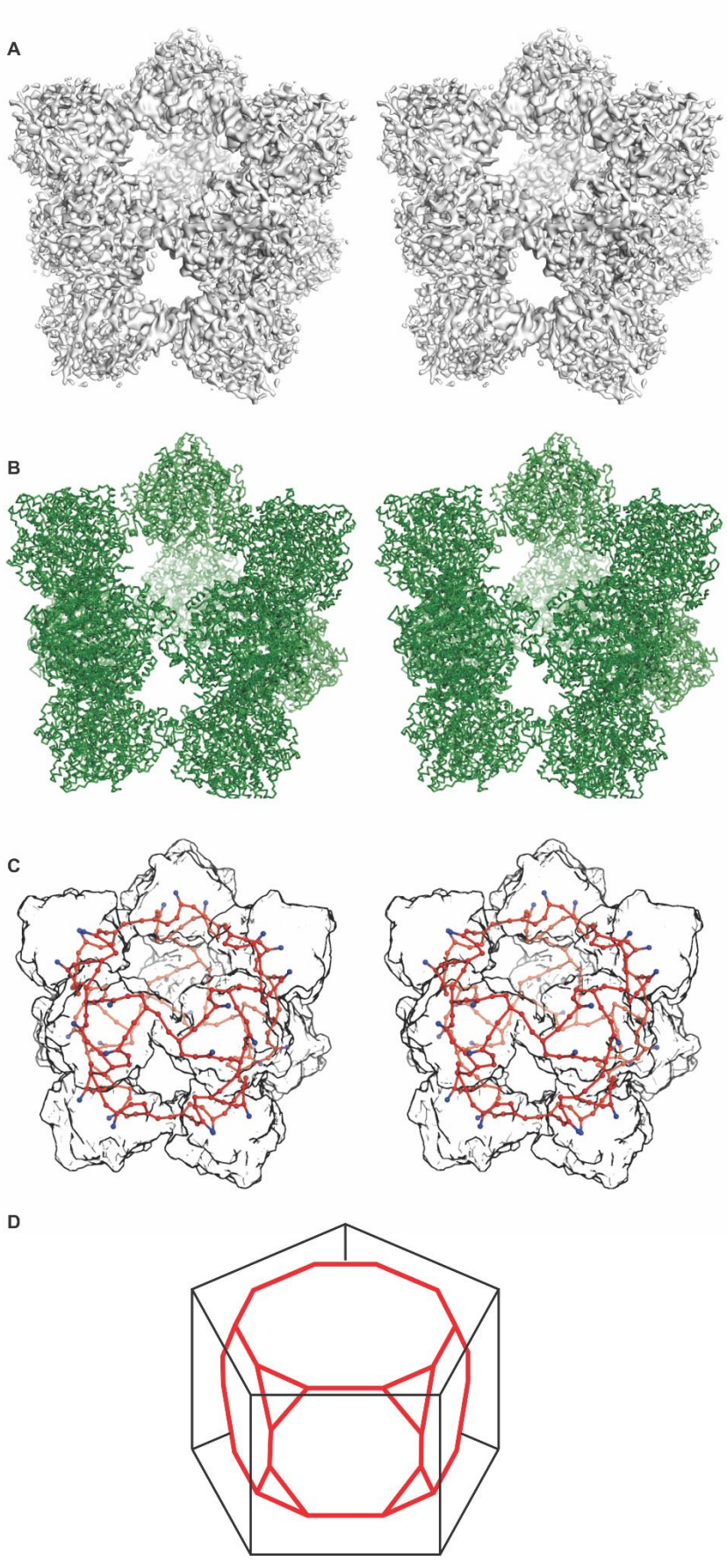
A
B
C
D

Fig. S7. Structure of 30-mer HDH particles. A. Stereo view of the 6.2 Å resolution cryo-EM map of 30-mer *K. stuttgartiensis* particles. B. Stereo figure showing a model of 30-mer *K. stuttgartiensis* HDH particles obtained by fitting HDH trimers from the crystal structure into the cryo-EM map. C. Stereo figure, showing the network of 240 hemes in the 30-mer HDH model. Each heme group is represented by its iron atom, shown as a red sphere (blue for active site heme irons). The surface of the HDH complex is shown as a black outline. D. The 240-heme network in the 30-mer roughly traces out a truncated pentagonal prism (red).

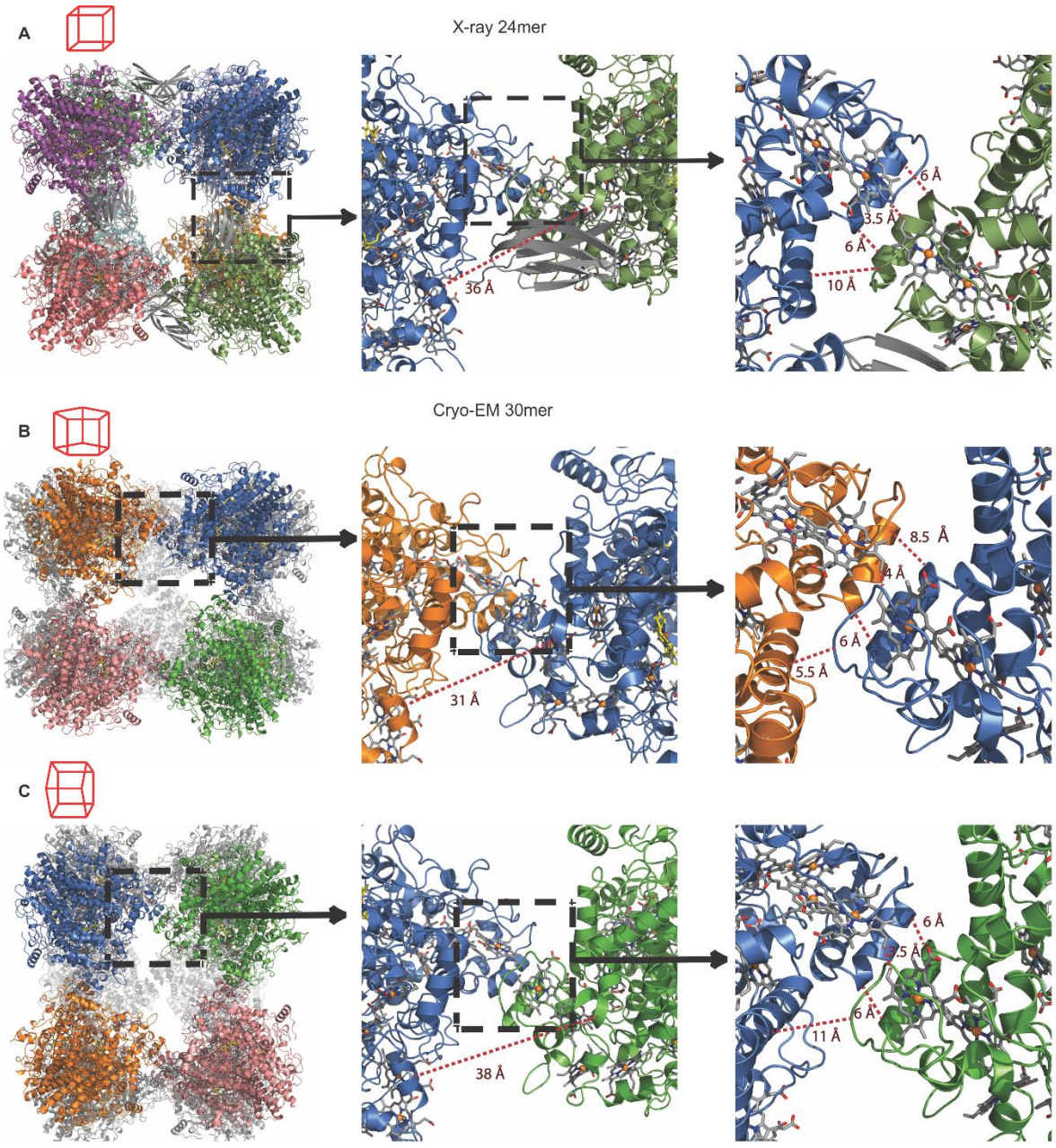

Fig. S8. Interactions in HDH assemblies. Interactions forming the various HDH oligomers observed without addition of Kustc1130. A. Because of the 432 point group symmetry, there is only one unique interface between HDH trimers in the 24-mer. B, C. In the 30-mer, which has 52 symmetry, two different interactions exist: between trimers within a pentameric ring (B) and between trimers belonging to different pentameric rings (C). These are highly similar to the interactions in the 24-mer, involving the same structural elements and differing only in the relative orientation of the interacting molecules.

Table S1. Data collection and refinement statistics.

	K. stuttgartiensis HDH (6HIF)
Data collection	
Space group	$P3_1$
Cell dimensions	
a, *b*, *c* (Å)	211.9, 211.9, 398.6
α, β, γ (°)	90.0, 90.0, 120.0
Resolution (Å)	185-2.8 (2.9-2.8)
R_{merge}	0.111 (0.745)
$I / \sigma I$	6.7 (1.2)
Completeness (%)	96.6 (98.8)
Redundancy	2.0 (2.1)
Refinement	
Resolution (Å)	185-2.8
No. reflections	452,098
R_{work} / R_{free}	22.2/23.9
No. atoms	
Protein	109094
Ligand/ion	8256 (heme) / 468 (other)
Water	935
B-factors	
Protein	64.2
Ligand/ion	52.8 (heme) / 96.0 (other)
Water	36.4
R.m.s. deviations	
Bond lengths (Å)	0.003
Bond angles (°)	0.949

*Values in parentheses are for the highest resolution shell.

Movie S1. Heme network in the HDH complex. Each heme group is represented by its iron atom, shown as a red sphere (blue for active site heme irons). The surface of the HDH complex is shown in white.